JOURNAL OF THE ROYAL SOCIETY Interface

A microfabricated wedge-shaped adhesive array displaying gecko-like dynamic adhesion, directionality and long lifetime

Aaron Parness, Daniel Soto, Noé Esparza, Nick Gravish, Matt Wilkinson, Kellar Autumn and Mark Cutkosky

J. R. Soc. Interface published online 18 March 2009
doi: 10.1098/rsif.2009.0048

JOURNAL OF THE ROYAL SOCIETY Interface

FirstCite® e-publishing

J. R. Soc. Interface
doi:10.1098/rsif.2009.0048
Published online

A microfabricated wedge-shaped adhesive array displaying gecko-like dynamic adhesion, directionality and long lifetime

Aaron Parness[1,*], Daniel Soto[2], Noé Esparza[1], Nick Gravish[3], Matt Wilkinson[3], Kellar Autumn[3] and Mark Cutkosky[1]

[1]*Department of Mechanical Engineering, Stanford University, Escondido Mall, Stanford, CA 94305, USA*
[2]*Department of Applied Physics, Stanford University, Via Pueblo Mall, Stanford, CA 94305, USA*
[3]*Department of Biology, Lewis and Clark College, Portland, OR 97219, USA*

Gecko adhesion has become a paradigmatic example of bio-inspired engineering, yet among the many gecko-like synthetic adhesives (GSAs), truly gecko-like performance remains elusive. Many GSAs have previously demonstrated one or two features of the gecko adhesive. We present a new wedge-shaped GSA that exhibits several gecko-like properties simultaneously: directional features; zero force at detachment; high ratio of detachment force to preload force; non-adhesive default state; and the ability to maintain performance while sliding, even after thousands of cycles. Individual wedges independently detach and reattach during sliding, resulting in high levels of shear and normal adhesion during drag. This behaviour provides a non-catastrophic failure mechanism that is desirable for applications such as climbing robots where sudden contact failure would result in serious falls. The effects of scaling patch sizes up to tens of square centimetres are also presented and discussed. Patches of 1 cm^2 had an adhesive pressure of 5.1 kPa while simultaneously supporting 17.0 kPa of shear. After 30 000 attachment/detachment cycles, a patch retained 67 per cent of its initial adhesion and 76 per cent of its initial shear without cleaning. Square-based wedges of 20 μm and 50 μm are manufactured in a moulding process where moulds are fabricated using a dual-side, dual-angle lithography process on quartz wafers with SU-8 photoresist as the mould material and polydimethylsiloxane as the cast material.

Keywords: gecko; adhesion; climbing; bio-inspired adhesive; fibrillar adhesion; scaling

1. INTRODUCTION

The gecko has inspired research by both biologists and engineers because of its ability to use a stiff material, β-keratin ($E \sim 1.6$ GPa) (Peattie *et al.* 2007), to create an effectively soft and tacky structure. Several important functional properties of the gecko adhesive were identified in 2005. The gecko adhesive is (i) directional, (ii) attaches strongly with minimal preload, (iii) detaches quickly and easily, (iv) sticks to nearly every material, (v) does not stay dirty or (vi) self-adhere, and (vii) is non-sticky by default (Autumn 2006). We believe another critical attribute of the gecko's adhesive is missing from this list: the ability to sustain high levels of adhesion while sliding. Because gecko setae and spatulae are able to independently detach and reattach, consistent levels of shear and normal adhesion are maintained as samples are dragged in their preferred direction across surfaces (Autumn *et al.* 2006*a*). The gecko employs this 'dynamic adhesion' to help engage and load the many terminal spatulae evenly. Dynamic adhesion also provides a non-catastrophic failure mechanism during climbing; feet gradually slip down the wall rather than losing adhesion suddenly.

The potential applications of gecko-like synthetic adhesives (GSAs) in robotics, biomedical devices, manufacturing and consumer products have spawned a large number of attempts to create usable materials. A compilation of the literature can be found in Fearing (2008). Although many of these synthetics have some gecko-like attributes, a structure that replicates all of the gecko adhesive's properties, and its subsequent use, remains a holy grail of sorts in the field. Table 1 summarizes the current state of these efforts, including the new microfabricated wedge-shaped adhesive reported in this paper.

Many groups have successfully exploited the contact-splitting aspect of the gecko adhesive (Geim *et al.* 2003; Yurdumakan *et al.* 2005; Tsai *et al.* 2006; Zhao *et al.* 2006;

*Author for correspondence (aaronparness@stanford.edu).

Received 4 February 2009
Accepted 13 February 2009

Table 1. GSA comparison.

	Gecko[a]; (Autumn *et al.* 2000; Gravish *et al.* 2007)	Parness Cutkosky	Schubert Fearing; Schubert *et al.* (2008)	Gorb *et al.* (2007)	Qu Dai; Qu *et al.* (2008)	Kim Sitti ; Kim & Sitti (2006)	Murphy Sitti; Murphy *et al.* (2008)	Santos Cutkosky; Santos *et al.* (2007)
adhesion (kPa)	48	5.1	0.3	60.6	100	180	80	2.4
shear stress (kPa)	184	25	0.9	N.M.	1000	N.M.	74	8.0
μ'	8–16	2.1	0.6	7.1	N.M.	1.5	7	13
test area (cm^2)	0.0093	1.0[b]	0.01	0.066	0.16	0.03	0.0044[c]	3.9
adhesive force (N)	0.45	0.51[b]	0.003	0.4	1.6	0.54	0.006[c]	1.0
durability (cycles)	$>30\,000$	$>30\,000$	>150	unknown	>2	unknown	unknown	>100
directional	yes	yes	—[d]	no	—[d]	no	yes	yes
zero-force detachment	yes	yes	yes	no	no	no	no	yes
non-adhesive default	yes	yes	yes	no	low	no	no	yes
dynamic adhesion	yes	yes	no	no	no	no	no	no

[a]Data presented are from tokay gecko setal arrays except μ', which uses single seta data.
[b]An 8.2 cm^2 patch was also tested yielding 2.1 N of adhesion and 13.0 N of shear (2.6 kPa adhesion and 15.9 kPa shear).
[c]A 1 cm^2 patch was also tested in pure shear by hanging a weight. This patch held 4.9 N statically in shear and 9.8 N quasi-statically in shear (49 kPa static shear and 98 kPa quasi-static shear, respectively).
[d]Non-directional features, but exhibits directional behaviour.

Ge *et al.* 2007). Interesting work has also been done on hierarchical structures and actively switchable adhesives (Northen & Turner 2005; Northen *et al.* 2008; Bhushan 2007). However, many of these structures were fabricated at right angles to the substrate despite the fact that real gecko setae are angled, permitting largely linear elastic deformation and low effective modulus (Autumn *et al.* 2006*c*). One recent GSA addressed directionality by fabricating fibres at an oblique angle to the substrate (Aksak *et al.* 2007). These angled pillars successfully lowered the effective stiffness of the sample and showed great promise, but the tips of the fibres were coplanar with the backing layer, creating a situation in which fibres probably pivot to a point contact after losing their initial contact. Tip shape has been shown to have a significant effect on adhesion for contact diameters greater than 1 μm (Gao & Yao 2004; del Campo *et al.* 2007), and non-directional synthetics using spatular tips (Kim & Sitti 2006; Gorb *et al.* 2007) achieved much greater adhesive pressures than the original angled GSAs. However, the latest work on angled stalks improved the tip geometry through a dipping procedure, dramatically increasing performance (Murphy *et al.* 2007, 2008). High aspect ratio, stiff polypropylene fibres have recently been shown to sustain high forces when loaded in shear by bending to create a side contact between the stalks and the surface (Lee *et al.* 2008; Schubert *et al.* 2008). Vertically aligned nanotubes with tangled tips have also been loaded in shear, creating side contacts between the nanotubes and surface, and producing high levels of shear and adhesion (Qu *et al.* 2008). Our group previously created an adhesive that combined directional stalks and non-coplanar tips (Santos *et al.* 2007; Kim *et al.* 2008) that performed well on a climbing robot (Kim *et al.* 2008), but this result was fabricated at a fibre diameter (d=380 μm) much larger than gecko setae, limiting its application to smooth surfaces and forcing the use of a soft material that is susceptible to fouling. Theory suggests that smaller features will generate higher levels of adhesion and that materials with a higher modulus of elasticity will resist clumping and fouling (Arzt *et al.* 2003; Dai *et al.* 2006; del Campo *et al.* 2007; Hui *et al.* 2007). Recent work has also shown increased adhesion on both wet and dry substrates through the use of surface coatings (Lee *et al.* 2007).

The adhesive presented here and pictured in figure 1 overcomes several recent challenges in the field of GSAs. During sliding in a flat punch test, 1 cm^2 samples retain approximately 100 per cent of their adhesion. Using a flat punch larger than the sample ensures that the same fibres are detaching and reattaching, whereas a spherical contact engages new fibres as it drags across a sample. Spherical probe tests have been used in the past because they do not require precise alignment, but it is unclear whether adhesion during sliding is due to new fibre engagement or the detaching and reattaching of the same fibres. Scaling the results of small spherical contact tests to large surface areas, while maintaining alignment, is also a challenge. Polypropylene fibres (Lee *et al.* 2008; Schubert *et al.* 2008) show continuous shear during drag, but require a positive normal force—a behaviour similar to kinetic friction. Data for the wedge-shaped adhesive are also consistent with the

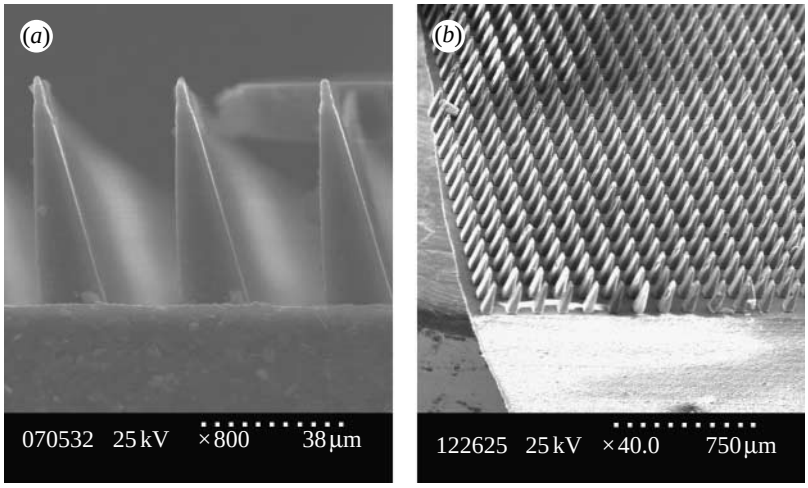

Figure 1. Scanning electron microscope images of microfabricated wedge-shaped adhesive array. (*a*) Side view of 20 µm base width by 80 µm height wedges and (*b*) diagonal view of a large array of 50 µm base width by 200 µm height wedges.

directional adhesion model of contact forces observed in the gecko (Autumn *et al.* 2006*a*). This means that adhesion increases when shear force is applied in a preferred direction, allowing the amount of adhesion to be controlled. Additionally, when the shear loading is removed, the adhesive can be detached with zero force. The sharp-tip shape helps engage the adhesive at low attachment forces and samples showed very long lifetime, retaining 67 per cent of their initial adhesion after 30 000 test cycles.

2. MATERIALS AND METHODS

2.1. Fabrication

Taking cues from previous work (Santos *et al.* 2007; Kim *et al.* 2008), a wedge shape was chosen as a simple anisotropic geometry with a sharp tip that would promote high levels of adhesion with low preload. For fabrication, we were inspired by work on angled microstructures unrelated to adhesion that used multiple angled exposures in SU-8 photoresist to create interesting three-dimensional geometries (Han *et al.* 2004; Sato *et al.* 2004; Yoon *et al.* 2006). Using thick films of SU-8, arrays of wedge-shaped cavities were created as a reusable mould for casting elastomeric polymers.

To create the SU-8 mould, a two-mask angled exposure technique was developed, for which an angled backside exposure was followed by a vertical topside exposure before development to create a three-dimensional structure in the film. Care was taken in the final mask designs to minimize volumes in the film that would be unmasked during both exposures. A custom-built tilting stage was used to orient the wafer at an angle under a collimated UV lamp for the angled exposure. This angle was chosen to account for SU-8's high index of refraction ($n=1.61$) (Hung *et al.* 2004). For the structures presented here, the target angle was 14.8° to create a 4 : 1 aspect ratio, which required an exposure angle of 23.5°. After the moulds were created, silicone-based elastomers were cast under vacuum, spun to a desired backing layer thickness, heat cured and pulled out of the mould by hand. Moulds typically exhibited reusability for over 10 cast and peel cycles before failing due to cracking, delamination from the wafer substrate or residual polymer clogging the mould cavities. The fabrication sequence is shown in figure 2.

The wedge-shaped adhesives were fabricated at two characteristic sizes with square base dimensions of 20 and 50 µm, and corresponding heights of 80 and 200 µm, respectively. The square bases were spaced to achieve a 25 per cent fill factor. In total, six sample types were fabricated and tested: 50 and 20 µm wedges of Silicones Inc. P-20; Dow Corning Sylgard 170; and Silicones Inc. P-70 polymer. Rectangular samples of the materials were tested in uniaxial tension using an Instron 5848 MicroTester (Instron Norwood, MA) to determine material properties. Each sample was stretched to 30 per cent strain at a ramp rate of 1.0 mm s^{-1}. The Young modulus was estimated to be linear for the region below 10 per cent strain and resulted in values of 440 kPa (P-20), 1.75 MPa (Sylgard 170) and 2.63 MPa (P-70). It was expected that the softest material, P-20, would show the strongest levels of adhesion, but would be susceptible to fouling and clumping.

Clumping is detrimental to the performance of a fibrillar adhesive. When adjacent fibres adhere to one another, the real area of contact between the adhesive and surface is reduced. An analysis similar to that described by Majidi *et al.* (2004) was performed to determine a clumping criterion by balancing deformation and surface energies. In this analysis, we included the shear strain term in the deformation energy to account for the small aspect ratio of the wedge. The wedge was approximated as a tapered beam characterized by the parameter α, where $\alpha=(w_0-w_1)/L$ and w_0 is the base width; w_L is twice the radius of curvature of the wedge's tip; and L is the height of the wedge. For a given spacing, base width and height, beams with a higher degree of taper have a higher tendency to clump, the reduction of deformation energy overcoming the increased tip to tip spacing produced by the taper. When using stiffer materials, deformation energy grows and the likelihood of clumping is reduced, as observed in our samples. Empirical observations

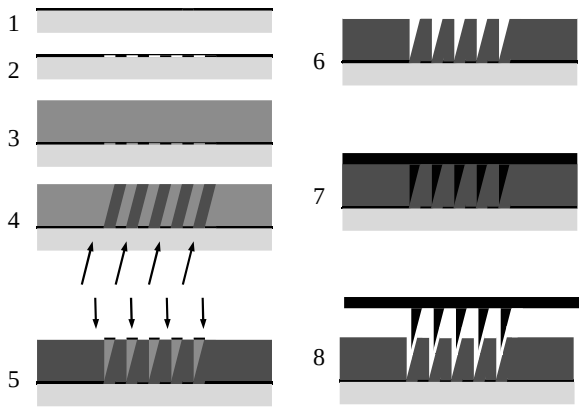

Figure 2. Fabrication sequence. (1) Deposit aluminium on UV transparent quartz wafer, (2) pattern aluminium to create self-aligned mask, (3) deposit SU-8 on top of aluminium, (4) angled self-aligned UV exposure from backside, (5) align mask to topside and UV expose, (6) develop, (7) cast and spin polydimethylsiloxane (PDMS) and (8) peel out cast adhesive structure and backing layer. Black, PDMS; light grey, quartz wafer; dark grey, exposed SU-8; grey, unexposed SU-8.

under a microscope showed the softest material, P-20, clumped at both the 50 and 20 μm wedge size, resulting in poor adhesive performance (figure 3). Arrays of stiffer Sylgard 170 and P-70 cast from the same mould, however, did not clump, but otherwise performed similar to each other despite differences in stiffness and surface energy, making direct comparisons difficult. All further data are for the Sylgard 170 material.

2.2. Test equipment and experimental methods

Data were collected using two different experimental test set-ups. Each set-up is capable of moving a flat glass substrate and sample into and out of contact along trajectories in both the normal and tangential directions simultaneously. Set-up 1 consists of a three-axis linear stage, force transducer and two-axis manual tilt stage. The motion stage (Velmex, MAXY4009W2-S4 and MA2506B-S2.5) has a 10 μm positioning resolution in the tangential direction and a 1 μm positioning resolution in the normal direction. A flat glass substrate is attached to the motion stage and the sample is placed upon a six-axis force/torque sensor (ATI Industrial Automation, Gamma Transducer SI-32-2.5) with an accuracy of approximately ± 25 mN. The force transducer is mounted onto a manual two-axis tilt stage (Newport, 30 Series Tilt Platform), which is used for manual alignment of the sample relative to the substrate. Set-up 2 is stiffer, slower and more precise. It consists of a two-axis linear stage, force transducer and two-axis tilt stage. The motion stage is formed by two Aerotech ANT-50L (Aerotech, Pittsburgh, PA) linear actuators, which provide positioning control on the nanoscale, and the flat glass substrate is attached rigidly to the motion stage. The sample is mounted onto a Kistler 9328A three-axis piezoelectric force sensor (Kistler, Winterthur, Switzerland). Two Newport goniometers, GON65L and TR120BL (Newport, Irvine, CA), are used to align the sample and substrate.

Three different types of experiments were performed, load–drag–pull (LDP), load–pull (LP) and longevity tests, as described further in §3. On set-up 1, force data were filtered using a low-pass third-order Butterworth filter with a cut-off frequency of 20 Hz. Experiments were designed to explore the dynamic adhesion, directionality and reusability properties of the microfabricated wedge-shaped adhesive arrays.

Figure 3. Typical clumping behaviour observed between adjacent stalks for very soft materials such as Silicones Inc. P-20. Stiffer materials did not exhibit extensive clumping.

3. RESULTS AND DISCUSSION

3.1. Dynamic adhesion

Data from a flat punch LDP test are shown in figure 4 (LDP tests consist of a 45° preload trajectory to a depth of 80 μm, followed by a 1 mm horizontal drag and finishing with a vertical pull-off; Autumn & Gravish 2008). These data are for a 1 cm^2 patch of 50 μm stalks made from Dow Corning Sylgard 170 silicone encapsulant with a backing thickness of 600 μm, but are representative of the results for all six sample types tested. The figure reveals a period of continuous adhesion during the 1 mm drag phase (between points 2 and 3 in figure 4). Unlike spherical indenter tests that engage new fibres as the probe moves horizontally across the sample, these data indicate that stalks must be detaching and reattaching since the entire patch is contacting during the duration of the test. The flat punch drag results for many previous GSAs, by contrast, pass through their peak adhesion (point 2 in figure 4) and immediately drop to near zero adhesion. The gecko also exhibits dynamic adhesion as shown in the flat punch LDP data for gecko setae (figure 5).

Dynamic adhesion, as observed in the gecko and with these samples, is valuable for climbing because failure becomes the onset of gradual sliding rather than

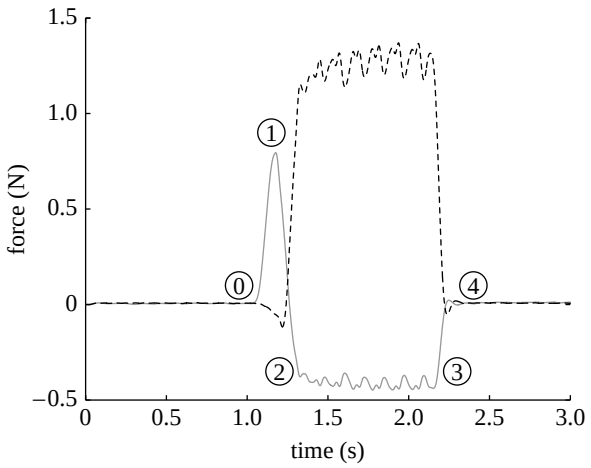

Figure 4. Wedge-shaped adhesive load–drag–pull (LDP) data from a single trial, 1 cm^2 patch size. Preload occurs from point 0 to 1 consisting of a 45° approach angle to a depth of 80 µm. This was followed by a 1 mm drag (points 2 and 3) and a vertical pull-off (points 3 and 4). The substrate moved at a constant 1 mm s^{-1} over the course of the trial. Note the sustained dynamic adhesion (solid curve) and shear (dashed curve) between points 2 and 3, indicating independent detachment and reattachment of single wedges.

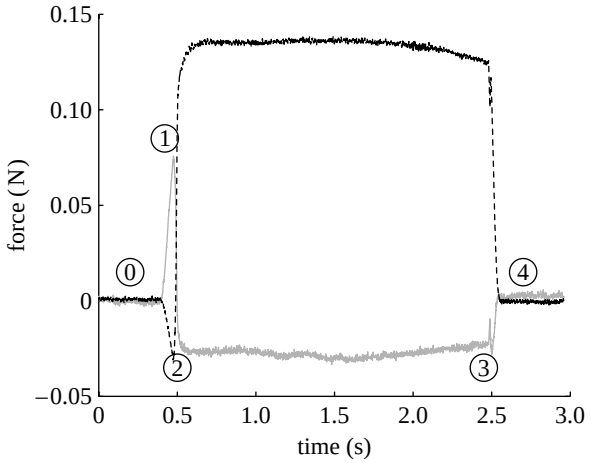

Figure 5. Gecko setae LDP data from a single trial. Comparison with figure 4 shows the strong behavioural similarity between the microfabricated wedge-shaped adhesive and gecko setae, especially the dynamic adhesion observed between points 2 and 3 (solid curve, adhesion; dashed curve, shear).

a catastrophic detachment event. A sliding contact failure allows time for an animal or robot to compensate by reattaching the slipping foot in another location or by placing additional feet on the surface. In geckos, the sliding phenomenon also helps to orient all of the terminal spatulae for good contact while not damaging individual contacting elements, and thereby reduces the demand on the accuracy of foot presentation to the climbing surface. A similar mechanism of sliding into a preferred orientation has recently been demonstrated in a GSA using carbon nanotubes with ribbon-like elements at the tips (Qu *et al.* 2008). We believe that spatulae distribute a load and self-align to their preferred orientation through sliding, relieving stress concentrations via frictional loss. Localized sliding could similarly help synthetic adhesives scale to larger patch sizes (discussed further in §4), and will be even more valuable to future versions of GSAs that are hierarchical and require a greater ability to passively distribute the load of a foot to individual contacts.

3.2. Directionality

Similar to the behaviour observed in individual gecko setae, setal arrays and whole gecko toes, the microfabricated wedge-shaped adhesive presented here follows the frictional adhesion model (Autumn *et al.* 2006*a*) by demonstrating more adhesion when loaded in a preferred shear direction. This property makes an adhesive particularly well suited to climbing vertical surfaces where the body weight of an animal or robot induces a large downward shear loading on the contacts, and where feet must be detached without disturbing the grip of the remaining legs.

Data were collected for the synthetic adhesive by running a series of flat punch LP tests (LP tests consist of a 45° angled preload that terminates at a depth ranging from 0 to 80% of the stalks' height followed by a 1 mm pull-off trajectory at a specified angle ranging from 0° to 180°). Shear and normal forces were recorded at the adhesive's failure point, and these data are plotted against each other in force space for the entire series in figure 6. The resulting representation is a limit surface in force space. Combinations of force above the curve formed by the data points are safe and the contact will be maintained; forces below the curve will result in contact failure. The limit surface plot shows the directional behaviour of the adhesive; maximum adhesion is reached only when a large value of shear is present. Additionally, because the limit surface intersects the origin, when no shear is applied to a sample, the adhesive detaches without any pull-off force in the normal direction. This phenomenon allows the structure to act as a *controllable adhesive* in which adhesion is controlled by varying the applied shear force. Efficient climbing relies on this behaviour. By contrast, materials such as pressure-sensitive adhesive tapes require a substantial preload to achieve adhesion and a similarly large force to achieve detachment. Robotic climbing with such materials is inefficient and also unreliable, because large detachment forces tend to create vibrations that cause other feet to lose their grip (Kim *et al.* 2008). Low detachment forces are also a critical feature of the rapid attachment/detachment cycles observed in the gecko (5 ms for attachment and 15 ms for detachment; Autumn *et al.* 2006*b*).

By contrast with the gecko, the wedge-shaped adhesive's data show bidirectional behaviour. While the gecko has a preferred shear direction, for which adhesion increases with shear loading, and an anti-preferred direction for which typical coulomb friction behaviour is observed, the wedge-shaped structure shows adhesion when loaded in either the upward or downward shear direction (lateral displacement results in purely frictional behaviour). This bidirectionality is visible in figure 6, which shows some symmetry across the y-axis. The symmetric behaviour can be attributed to the thin tip at the end of the wedge, which is capable

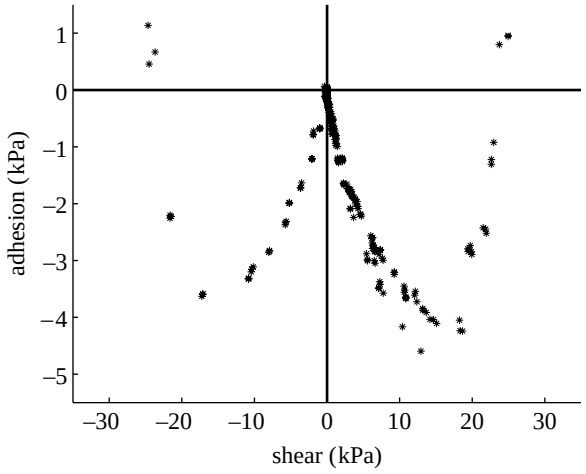

Figure 6. Limit surface of a Sylgard 170 sample of 50 μm base width wedges on a 225 μm backing layer, 1 cm^2 patch size. Points indicate contact failures either through slipping or detachment from the surface. Important to note: adhesion is achieved only in the presence of shear loading, following the frictional adhesion model (Autumn *et al.* 2006*a*). Also, the limit surface intersects the origin, indicating that, when no shear is present, the adhesive can be detached with zero force.

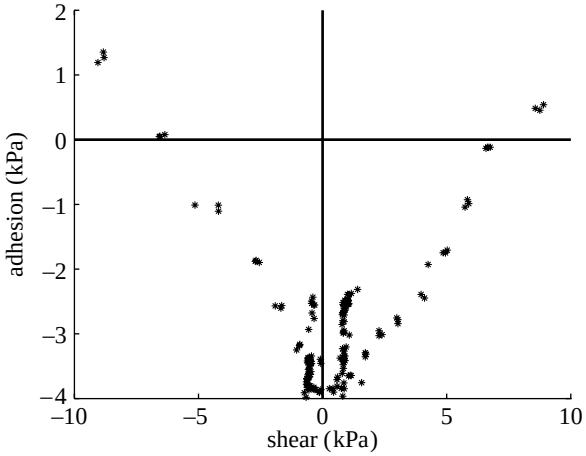

Figure 7. Limit surface of a flat sample of Sylgard 170. This set of data follows the embedded friction cone model exhibiting the strongest adhesion when no shear loads are present.

of flopping over in the anti-preferred direction and creating a significant area of contact when loaded in such a way. However, the desirable functions of directionality are maintained: (i) adhesion increases with shear loading and (ii) the force limit surface passes through the origin. By contrast, for a curved elastic shape described by the Johnson–Kendall–Roberts adhesion model for a sphere contacting a flat surface (Johnson *et al.* 1971), the opposite behaviour would be predicted: (i) adhesion would decrease with shear loading and (ii) the adhesion would be maximal at zero shear load. Compared with the gecko's adhesive, the wedge-shaped adhesive structure has a smaller angular range over which zero-force detachment occurs, but it is present for approximately $\pm 10°$ with respect to vertical pull-off. For reference, flat control patches were tested with the same trajectories and the results are shown in figure 7. These data approximately match Johnson–Kendall–Roberts behaviour.

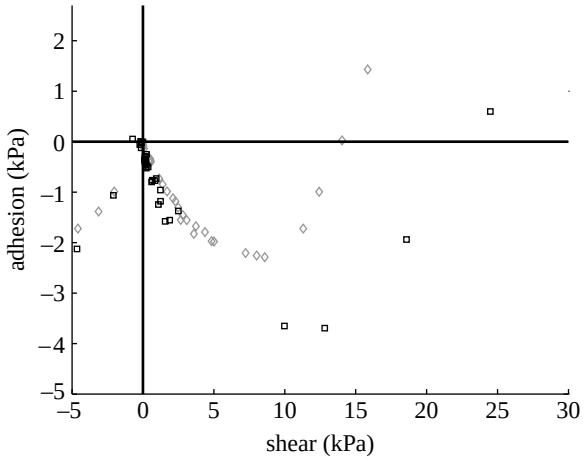

Figure 8. Comparison of arrays of 20 μm base width (squares) and 50 μm base width (diamonds) wedges. Patch size of 1 cm^2 and backing layer thickness of 600 μm. Trajectories were scaled to wedge size.

While easy detachment of feet is crucial to climbing quickly and efficiently, easy attachment is equally important. The gecko, using a many-tiered hierarchy, exhibits a value of μ' (the ratio of pull-off force to preload force) between 8 and 16 depending on conditions (Autumn *et al.* 2000), meaning that it can press its foot to a surface with 1 N of force and generate 8–16 N of adhesion. Published μ'-values for GSAs range from below 0.1 to as high as 7.5 (Gorb *et al.* 2007) and 13 (Santos *et al.* 2007). The highest μ' observed for the wedge-shaped adhesive was 2.1 and occurred when wedges were loaded at an incoming angle of 30° to avoid buckling. Adhesion during this trial was 4.9 kPa, very near the maximum adhesive pressure observed. Minimizing the required preload is important for climbing applications. Depending on where the feet are placed, a minimum value of $\mu' \approx 0.33$ is needed for a quadruped, so that the attached feet can produce sufficient force to preload a new foot as it is brought into contact.

Results for similar patches fabricated from Sylgard 170 at both the 20 and 50 μm base width are plotted in figure 8. Both samples were 1 cm^2 patches with 600 μm backing layers. When subjected to the same loading trajectory scaled by the wedge size (i.e. a penetration depth of 40 μm for a 20 μm base width wedge and a penetration depth of 100 μm for a 50 μm base width wedge), the arrays have the same real area of contact, but with a 2.5× increase in the summed perimeter of the contacting elements for the smaller wedge size. It has been reasoned that contact splitting will increase overall adhesion in a vertical preload/vertical pull-off experiment (Arzt *et al.* 2003), and similar behaviour is observed in figure 8 for our directional tests. The backing layer thickness was also found to have a significant effect on adhesive pressures as predicted by Kim *et al.* (2007), with thin backing layers performing better. The sample patch size was another factor that influenced adhesive performance because of scaling effects, so backing thickness and patch size were normalized for the size comparison tests. Further research is ongoing on a broader variety of materials

and feature sizes to generate more conclusive comparisons among bulk stiffness, feature size, backing thickness and overall levels of adhesion. However, the general directional behaviour of the stalks, their ability to adhere dynamically, and the shape of the contact limit surface remained consistent at both characteristic sizes across all trials.

3.3. Long lifetime

Among its desirable properties, the gecko's adhesive system is highly reusable, as it must climb for long periods of time before new growth replaces the setae and terminal spatular elements of its toe pads. Comparatively few results have been presented in the literature on the reusability of GSAs. Where data are presented, the performance often drops significantly after a few tests because structures have broken or become dirty (Geim *et al.* 2003; Northen & Turner 2005; Yurdumakan *et al.* 2005; Kim & Sitti 2006; Zhao *et al.* 2006; Aksak *et al.* 2008). Some exceptions are the large-angled stalks previously fabricated in our laboratory (Santos *et al.* 2007) and one type of mushroom-shaped adhesive (Gorb *et al.* 2007), which demonstrate reusability for over 100 attachment/detachment cycles before performance degrades and cleaning is required. After this cleaning, some samples were shown to regain their initial performance. Stiff polypropylene hairs (Lee *et al.* 2008; Schubert *et al.* 2008) also retained a high level of performance for over 150 cycles, even showing an increase in performance due to a 'breaking in' of fibres. The microfabricated wedge-shaped adhesive reported here maintained 67 per cent of its initial adhesion and 76 per cent of initial shear after 30 000 trials, without cleaning before the experiment was arbitrarily stopped.

Figure 9 shows data for a 1 cm^2 patch of wedge-shaped adhesive with a 50 µm square base cast from Sylgard 170 over a battery of 30 000 LDP cycles. The drag phase of these tests was extended from 1 to 10 mm in order to increase the rate of wear on the stalks. A preload depth of 100 µm was used, and the maximum values of shear and normal adhesion during the drag phase were taken as data points from every 1000th trial and plotted.

A high value of μ' can enhance reusability by preventing damage to stalks during the loading procedure. In the case of our synthetic adhesive, durability is also a result of the elastomeric material's ability to bend and deform without fracturing or tearing. A gecko's adhesive system is massively reusable (also over 30 000 trials) with a very stiff material, β-keratin, and at stresses much greater than those sustained by the synthetic adhesive. The gecko achieves this result, in part, because of its multilevel hierarchy that distributes the load evenly to individual spatulae and it generates such high levels of adhesion because of the more optimal spatular contact shape and size. Setae and spatulae also avoid overload damage by detaching and resticking as needed. A similar dynamic adhesion property was observed in the wedge-shaped adhesive as discussed in §1. Without these attributes, it is not surprising that non-sliding GSAs using stiff

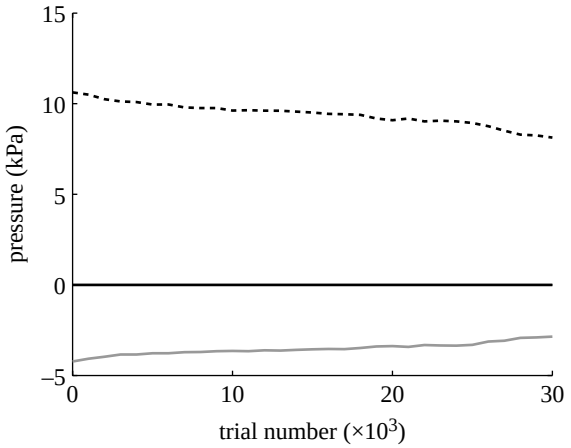

Figure 9. Lifetime data for a single sample of 50 µm base width wedges made from Sylgard 170, patch size 1 cm^2. The wedge-shaped adhesive retained over 67% of their initial adhesion (solid line) and 76% of their initial shear (dashed line) after 30 000 trials.

materials without a hierarchy of structural elements show high levels of adhesion for only a few tests. For future GSAs to achieve both high adhesion and durability, they will require a mechanism for even load distribution and an optimized contact structure.

4. SCALING ARRAY SIZE

Much of the early work on GSAs focused on the creation of fibrillar structures at the micro- and nanoscales. Many of these GSAs were tested using atomic force microscopes or micro-scale systems that measured the adhesion of samples of the order of several square millimetres or less. As the understanding of fibrillar adhesive systems has broadened, there has been more focus on creating larger arrays of more complex directional features and testing samples of the order of several square centimetres. Interest in GSAs for commercial and industrial uses may push patch sizes even larger. However, adhesive forces do not generally scale linearly with patch area due to several factors including alignment, uniformity and loading/unloading challenges.

One major obstacle that prevents the use of large patches is alignment. As an example, a fibrillar adhesive patch whose features are tolerant to ±20 µm of variation in the normal direction (this is approx. accurate for the smaller size of microfabricated wedge-shaped adhesive presented in this paper) would be effective for angular misalignments less than 1.15° across a 1 mm×1 mm patch, 0.115° across a 1 cm×1 cm patch and only 0.0115° across a 10 cm×10 cm patch. This level of alignment accuracy is challenging to achieve in a rigid experimental set-up, and becomes impossible in an uncontrolled environment. This analysis also assumes a perfectly flat substrate and a perfectly flat sample, which is often not the case due to variations in the backing layer thickness or variations in fibre height. These challenges were confronted in practice when the wedge-shaped adhesive structures were applied to a 500 g climbing robot platform

(Kim *et al.* 2008). Although the wedge-shaped adhesive demonstrated more adhesion on the rigid experimental set-up than the much larger features originally used on the robot (Santos *et al.* 2007), only stationary hanging was achieved because much of the adhesive patch failed to make close contact with the climbing surface (observed visually due to a change in the reflected light from contacting features). The robot's original stalks have a height of over 1 mm, requiring much less angular accuracy during foot placement. Approximately 100 per cent of these larger stalks engaged across the 4 cm^2 toe during climbing as opposed to regions of 5–25% of the wedge-shaped adhesive patches during stationary hanging.

Another challenge in applying GSAs to robots or other macroscale applications is the prevention of peeling. If a patch begins to peel at one corner or edge, the stress concentration can quickly propagate across the entire patch, resulting in a complete adhesive failure. While fibrous adhesive structures inherently have some crack trapping ability (Glassmaker *et al.* 2007), a zipper-like effect will still occur with a sufficiently large peeling moment. The soft elastomeric material can also stretch within the backing layer and induce a stress concentration on a single row of stalks, causing sequential detachment of all rows. This type of peeling has been observed under misaligned loading conditions for patches of the wedge-shaped adhesive structures that lack a stiff backing. Future generations of GSAs can take further inspiration from the gecko and create hierarchical systems that self-align to surfaces and promote equal load sharing to prevent the initiation of peeling. Also, the use of stiffer bulk materials can further prevent peeling by reducing the stresses created when the backing layer stretches.

Figure 10 shows the results of multiple samples of the wedge-shaped adhesive taken from the same mould, cut to various areas ranging from 0.1 to 8.2 cm^2, and tested on set-up 1. These samples were all cast out of Sylgard 170 with a uniform 300 µm backing layer. The first set of data shows the adhesive pressures for a fixed trajectory that does not cause high preload forces (45° preload angle, 120 µm preload depth and 150° pull-off angle). These data indicate a significant drop off in adhesion as patch size increases. A second set of data shows the maximum adhesive pressures achieved for any preload depth and pull-off angle. The adhesion pressures are higher than the fixed trajectory dataset, and show a somewhat less dramatic drop as patch size increases. However, to achieve these maximum pressures requires much higher preload pressures, effectively overcoming alignment challenges by smashing the sample and glass surface together to assure that a high number of wedges make contact. For the smaller patch sizes in these experiments, a high percentage of stalks make good contact under light preload pressure because alignment is not as challenging, but, for the larger samples, the initial percentage of wedges in good contact is much lower and can be improved significantly by increasing the preload pressure to force more wedges into contact. This tactic drastically reduces the μ'-value, making it less desirable for use in climbing applications where preload forces are

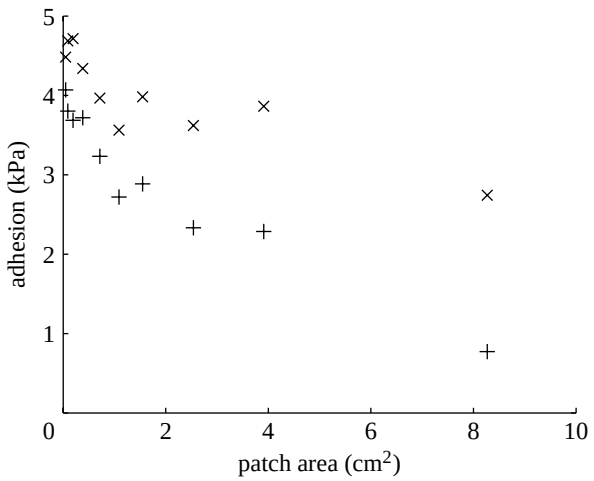

Figure 10. Adhesion pressures for various patch sizes. All samples were taken from the same mould and have a 300 µm backing layer thickness. Identical trajectories consisting of a 45° preload to a depth of 120 µm followed by a 150° pull-off were used for the fixed preload (pluses) dataset. The maximum adhesive pressures (crosses) are also presented. These data occurred at higher preload depths ranging from 140 to 180 µm. Using a higher preload helps to overcome misalignments in the contact between wedges and the glass substrate. This tactic, however, is impractical for climbing applications where the ability to apply preload forces is limited.

difficult to generate. Larger samples were also anecdotally more difficult to align in the test bed and had greater test-to-test variability. Trends such as these make macroscale adhesive projections from atomic force microscope data or small spherical probe apparatuses unfair. Likewise, predictions of this adhesive's potential performance of the order of hundreds or thousands of Newtons of adhesion are unrealistic from the data presented in this paper.

For adhesive applications that require areas larger than that of a 100 mm wafer, tiling of microstructured patches may be necessary. Fidelity of the wedge-shaped adhesive features was good across the entirety of a 100 mm wafer, but the effects of tiling several patches together into one larger patch have not been investigated. Foreseeable issues with this approach include the possible introduction of stress concentrations at the boundaries of individual tiles, and increased difficulty in aligning several patches to contact the surface simultaneously, especially if the backing thickness of these patches is not carefully controlled.

5. CONCLUSION

Wedge-shaped adhesive arrays were fabricated using a dual exposure lithographic mould making process using silicone rubbers as the cast material. The adhesive shares several desirable adhesive properties with the gecko, making it a promising step for climbing robots and related applications. In particular, the wedge-shaped adhesive is directional, displays dynamic adhesion, and is reusable for over 30 000 attach/detach cycles. Maximum forces were measured at 2.1 N in the normal direction and 13 N in shear direction for an 8.2 cm^2 patch. Typical results from 1 cm^2 patches

yielded more than 5 kPa and more than 17 kPa of normal and shear pressure simultaneously with a μ' larger than 2. For larger patches, the adhesion and shear pressure reduced gradually. Despite this promising performance on experimental test platforms, when the adhesive was applied to a 500 g climbing robot (Kim *et al.* 2008), only stationary hanging was achieved because much of the adhesive patch failed to make close contact with the climbing surface. More broadly, many GSAs have now been fabricated with enough adhesion for use in climbing. However, the practical application of these materials is inhibited by several factors. Some GSAs still lack directionality and zero-force detachment, making them poor candidates for climbing. But even GSAs that possess these properties fail to self-align and distribute the load evenly to individual fibres when scaled to patch sizes of several square centimetres and beyond, causing the demands on alignment and uniformity to be exceedingly great. The gecko employs a multistage hierarchy that ensures intimate contact between the nanoscale spatulae and the climbing surface without precise foot alignment or attachment trajectories. While improvements to the basic wedge design are being pursued, much of our current and future work focuses on a hierarchical suspension, similar to the gecko's, which will allow directional microfabricated adhesives to work in the macroscale world outside the laboratory.

This work was performed in part at the Stanford Nanofabrication Facility of NNIN, supported by the National Science Foundation under grant no. ECS-9731293. The work was supported in part by DARPA-Zman, the NSF Center of Integrated Nanomechanical Systems (COINS), the CIS New Users Grant Program and NSF NIRT (UCSB).

REFERENCES

Aksak, B., Murphy, M. & Sitti, M. 2007 Adhesion of biologically inspired vertical and angled polymer microfiber arrays. In *IEEE Int. Conf. on Robotics and Automation, Pasadena, CA, USA, 19–23 May 2008.* (doi:10.1021/la062697t)

Aksak, B., Murphy, M. & Sitti, M. 2008 Gecko inspired micro-fibrillar adhesives for wall climbing robots on micro/nanoscale rough surfaces. *IEEE Int. Conf. Robot. Autom.* **23**, 3322–3332.

Arzt, E., Gorb, S. & Spolenak, R. 2003 From micro to nano contacts in biological attachment devices. *Proc. Natl. Acad. Sci. USA* **100**, 10 603–10 606. (doi:10.1073/pnas.1534701100)

Autumn, K. 2006 Properties, principles, and parameters of the gecko adhesive system. In *Biological adhesives* (eds A. Smith & J. Callow), pp. 225–256. Berlin, Germany: Springer.

Autumn, K. & Gravish, N. 2008 Gecko adhesion: evolutionary nanotechnology. *Phil. Trans. R. Soc. A* **366**, 1575–1590. (doi:10.1098/rsta.2007.2173)

Autumn, K., Liang, Y. A., Hsieh, S. T., Zesch, W., Chan, W. P., Kenny, T. W., Fearing, R. & Full, R. J. 2000 Adhesive force of a single gecko foot-hair. *Nature* **405**, 681–685. (doi:10.1038/35015073)

Autumn, K., Dittmore, A., Santos, D., Spenko, M. & Cutkosky, M. 2006*a* Frictional adhesion: a new angle on gecko attachment. *J. Exp. Biol.* **209**, 3569–3579. (doi:10.1242/jeb.02486)

Autumn, K., Hsieh, S. T., Dudek, D. M., Chen, J., Chitaphan, C. & Full, R. J. 2006*b* Dynamics of geckos running vertically. *J. Exp. Biol.* **209**, 260–272. (doi:10.1242/jeb.01980)

Autumn, K., Majidi, C., Groff, R. & Dittmore, A. 2006*c* Effective elastic modulus of isolated gecko setal arrays. *J. Exp. Biol.* **209**, 3558–3568. (doi:10.1242/jeb.02469)

Bhushan, B. 2007 Adhesion of multi-level hierarchical attachment systems in gecko feet. *J. Adhes. Sci. Technol.* **21**, 1213–1258. (doi:10.1163/156856107782328353)

Dai, Z., Yu, M. & Gorb, S. 2006 Adhesion characteristics of polyurethane for bionic hairy foot. *J. Intell. Mater. Syst. Struct.* **17**, 734–741. (doi:10.1177/1045389X06055829)

del Campo, A., Greiner, C. & Arzt, E. 2007 Contact shape controls adhesion of bioinspired fibrillar surfaces. *Langmuir* **23**, 10 235–10 243. (doi:10.1021/la7010502)

Fearing, R. 2008 *Gecko adhesion bibliography.* Department of EECS, University of California, Berkeley, See http://robotics.eecs.berkeley.edu/~ronf/Gecko/gecko-biblio.html.

Gao, H. & Yao, H. 2004 Shape insensitive optimal adhesion of nanoscale fibrillar structures. *Proc. Natl. Acad. Sci. USA* **101**, 7851–7856. (doi:10.1073/pnas.0400757101)

Ge, L., Sethi, S., Ci, L., Ajayan, P. & Dhinojwala, A. 2007 Carbon nanotube-based synthetic gecko tapes. *Proc. Natl. Acad. Sci. USA* **104**, 10 792–10 795. (doi:10.1073/pnas.0703505104)

Geim, A., Dubonos, S., Grigorieva, I., Novoselov, K., Zhukov, A. A. & Shapoval, S. Yu. 2003 Microfabricated adhesive mimicking gecko foot-hair. *Nat. Mater.* **2**, 461–463. (doi:10.1038/nmat917)

Glassmaker, N., Jagota, A., Hui, C., Noderer, W. & Chaudhury, M. 2007 Biologically inspired crack trapping for enhanced adhesion. *Proc. Natl. Acad. Sci. USA* **104**, 10 786–10 791. (doi:10.1073/pnas.0703762104)

Gorb, S., Varenberg, M., Peressadko, A. & Tuma, J. 2007 Biomimetic mushroom-shaped fibrillar adhesive microstructure. *J. R. Soc. Interface* **4**, 271–275. (doi:10.1098/rsif.2006.0164)

Gravish, N., Wilkinson, M. & Autumn, K. 2007 Frictional and elastic energy in gecko adhesive detachment. *J. R. Soc. Interface* **5**, 339–348. (doi:10.1098/rsif.2007.1077)

Han, M., Lee, W., Lee, S. K. & Lee, S. S. 2004 3D microfabrication with inclined/rotated UV lithography. *Sens. Actuat. A Phys.* **111**, 14–20. (doi:10.1016/j.sna.2003.10.006)

Hui, C., Jagota, A., Shen, L., Rajan, A., Glassmaker, N. & Tang, T. 2007 Design of bio-inspired fibrillar interfaces for contact and adhesion—theory and experiments. *J. Adhes. Sci. Technol.* **21**, 1259–1280. (doi:10.1163/156856107782328362)

Hung, K.-Y., Hu, H. T. & Tseng, F. G. 2004 Application of 3D glycerol-compensated inclined-exposure technology to an integrated optical pick-up head. *J. Micromech. Microeng.* **14**, 975–983. (doi:10.1088/0960-1317/14/7/019)

Johnson, K., Kendall, K. & Roberts, A. 1971 Surface energy and the contact of elastic solids. *Proc. R. Soc. A* **324**, 301–313. (doi:10.1098/rsif.2007.1077)

Kim, S. & Sitti, M. 2006 Biologically inspired polymer microfibers with spatulate tips as repeatable fibrillar adhesives. *Appl. Phys. Lett.* **89**, 261 911. (doi:10.1063/1.2424442)

Kim, S., Sitti, M., Hui, C. Y., Long, R. & Jagota, A. 2007 Effect of backing layer thickness on adhesion of single-level elastomer fiber arrays. *Appl. Phys. Lett.* **91**, 161 905. (doi:10.1063/1.2801371)

Kim, S., Spenko, M., Trujillo, S., Heyneman, B., Santos, D. & Cutkosky, M. R. 2008 Smooth vertical surface climbing with directional adhesion. *IEEE Trans. Robot.* **24**, 65–74. (doi:10.1109/TRO.2007.909786)

Lee, H., Lee, B. P. & Messersmith, P. B. 2007 A reversible wet/dry adhesive inspired by mussels and geckos. *Nature* **448**, 338–341. (doi:10.1038/nature05968)

Lee, J., Majidi, C., Schubert, B. & Fearing, R. 2008 Sliding-induced adhesion of stiff polymer microfibre arrays. I. Macroscale behaviour. *J. R. Soc. Interface* **5**, 835–844. (doi:10.1098/rsif.2007.1308)

Majidi, C., Groff, R. & Fearing, R. 2004 Clumping and packing of hair arrays manufactured by nanocasting. In *ASME Int. Mechanical Engineering Congress & Exposition, Anaheim, CA, USA, 13–19 November 2004*.

Murphy, M. P., Aksak, B. & Sitti, M. 2007 Adhesion and anisotropic friction enhancements of angled heterogeneous micro-fiber arrays with spherical and spatula tips. *J. Adhes. Sci. Technol.* **21**, 1281–1296. (doi:10.1163/156856107782328380)

Murphy, M. P., Aksak, B. & Sitti, M. 2008 Gecko-inspired directional and controllable adhesion. *Small* **5**, 170–175. (doi:10.1002/smll.200801161)

Northen, M. & Turner, K. 2005 A batch fabricated biomimetic dry adhesive. *Nanotechnology* **16**, 1159–1166. (doi:10.1088/0957-4484/16/8/030)

Northen, M. T., Greiner, C., Arzt, E. & Turner, K. L. 2008 A gecko-inspired reversible adhesive. *Adv. Mater.* **20**, 3905–3909. (doi:10.1002/adma.200801340)

Peattie, A., Majidi, C., Corder, A. & Full, R. 2007 Ancestrally high elastic modulus of gecko setal β-keratin. *J. R. Soc. Interface* **4**, 1071–1076. (doi:10.1098/rsif.2007.0226)

Qu, L., Dai, L., Stone, M., Xia, Z. & Wang, Z. 2008 Carbon nanotube arrays with strong shear binding-on and easy normal lifting-off. *Science* **322**, 238–242. (doi:10.1126/science.1159503)

Santos, D., Spenko, M., Parness, A., Kim, S. & Cutkosky, M. 2007 Directional adhesion for climbing: theoretical and practical considerations. *J. Adhes. Sci. Technol.* **21**, 1317–1341. (doi:10.1163/156856107782328399)

Sato, H., Houshi, Y. & Shoji, S. 2004 Three-dimensional micro-structures consisting of high aspect ratio inclined micro-pillars fabricated by simple photolithography. *Microsyst. Technol.* **10**, 440–443. (doi:10.1007/s00542-004-0400-9)

Schubert, B., Lee, J., Majidi, C. & Fearing, R. S. 2008 Sliding-induced adhesion of stiff polymer microfibre arrays. II. Microscale behaviour. *J. R. Soc. Interface* **5**, 845–853. (doi:10.1098/rsif.2007.1309)

Tsai, Y., Shih, W., Wang, Y., Huang, L. & Shih, P. 2006 E-beam photoresist and carbon nanotubes as biomimetic dry adhesives. In *Proc. 19th IEEE Int. Conf. on Micro Electro Mechanical Systems, Istanbul, Turkey*, pp. 926–929. (doi:10.1109/MEMSYS.2006.1627952)

Yoon, Y., Park, J. & Allen, M. 2006 Multidirectional UV lithography for complex 3-D MEMS structures. *Microelectromech. Syst.* **15**, 1121–1130. (doi:10.1109/JMEMS.2006.879669)

Yurdumakan, B., Raravikar, N., Ajayan, P. & Dhinojwala, A. 2005 Synthetic gecko foot-hairs from multiwalled carbon nanotubes. *Chem. Commun.* **2005**, 3799–3801. (doi:10.1039/b506047h)

Zhao, Y., Tong, T., Delzeit, L., Kashani, A., Meyyappan, M. & Majumdar, A. 2006 Interfacial energy and strength of multiwalled-carbon-nanotube-based dry adhesive. *J. Vac. Sci. Technol. B Microelectron. Nanometer Struct.* **24**, 331–335. (doi:10.1116/1.2163891)